Non-linear Modal Behaviour in Cantilever Beam Structures

<u>Thamthada Suwanwong</u> and Paul.W.Bland*

Department of Mechanical Engineering Simulation & Design,

The Sirindhorn International Thai-German Graduate School of Engineering (TGGS),

King Mongkut's University of Technology North Bangkok, Bangkok 10800, Thailand (KMUTNB).

* Corresponding Author: Tel: +66 (0) 2913 2500 ext. 2915, Fax: +66 (0) 2913 2500 ext. 2922,

E-mail: bland.p.mesd@tggs-bangkok.org

Abstract

Modal analysis theory is based on linear assumptions, yet even relatively simple real structures exhibit non-linear (NL) behaviour. The objective of this work was to excite and detect NL modal behaviour in simple single and sandwich cantilevered beam structures composed of aluminium and rubber layers.

Standard modal testing and analysis was performed on all beam configurations using the impulse hammer excitation method, using a range of excitation force levels. The resulting Frequency Response Functions (FRF) were compared, as the main indicator of NL behaviour, most importantly by looking for changes in the peak amplitude and frequency for a given mode. A linear Finite Element (FE) model was used to give a baseline validation against static tests and modal test data using cases with the least evidence of NL behaviour, allowing the rubber layer properties to be modelled, at least for linear behaviour assumptions. All remaining beam configurations were then modelled using these material properties, and compared to test results in order to further identify NL behaviour.

The FE model showed no shift in peak amplitude or frequency for any mode for changes in the excitation force level, as expected for a linear model. All beam configurations showed evidence of NL behaviour from the modal tests, with the FRF modes peak amplitudes and frequencies shifting for changes in the excitation force level. All modes for all sandwich beam configurations showed decreasing peak amplitude and frequency, for increasing excitation force. The peak amplitude and frequencies for single beam configurations showed a mix response to increasing the excitation force, with some modes increasing, some remaining unchanged, some decreasing and some not showing any clear trend.

Key words: Modal analysis, non-linear, beams

1. Introduction

The background theory and application of modal testing and modal analysis is well established and a powerful tool [1,2]. However, due to increasing demands of measurement and simulation capability and accuracy driven by trends such as engineering component and assembly increasing complexity, optimisation, performance, smaller dimensional scales, computational power and multiphysics type problems, its key limitation is that traditional modal analysis is based on linear assumptions.

All real structures are fundamentally NL, even if only for the simple reason that for a sufficiently large displacement the mathematics contains NL terms. Recommended background reading, including types and sources of NL, is given here [3,4].

A comprehensive review was published in 2006 (88 pages, 446 references) on NL structural dynamics by Kerschen et al [5], and therefore not repeated here. The authors have not found an updated review since that date, although the research area continues to be very active and is arguably still maturing. Some examples are briefly given as follows. Lee et al. [6] investigated the NL behaviour of a multiphysics system, the application being aircraft stability and control, part of which is the modal NL analysis of structures and aeroelastic instability. Peeters et al. [7] assessed the robustness of an experimental technique for a single cantilevered beam configuration with an added geometric non-linearity, to identify NL behaviour, based on the phase resonance methodology and using sine step and free decay methods. Carrella and Ewins [8] proposed an approximate solution for engineering scale applications, based on a single degree of freedom (SDOF) method extracting standard parameters from a measured FRF for a fixed response amplitude, and then repeated at different amplitudes. Whilst this does not in any way change any of the already existing modal analysis linear approach, it is a type of linearization, allowing empirical relationships between the natural frequencies and damping ratios as functions of the response amplitude, and therefore offers an "engineering" solution. Mahmoodi et al [9] studied a cantilevered

sandwich beam with two high carbon content steel beams sandwiching an epoxy resin layer with various % content of carbon nano-tubes, observing a change of resonant frequency linked to excitation amplitude level. This will become increasingly relevant for emerging modern engineering materials.

In general, the experimental work reported in any given paper tends to be applied to a limited number of beam configurations or beam composition variables. Therefore the work present here is a first step in investigating the effects of structural, material and test parameters that promote NL behaviour, critically by experimental work that excites and identifies such behaviour using single and sandwich beams with a wide range of configurations.

2. Methodology

Experimental modal analysis was performed on single and multiple layered cantilevered beams composed of aluminium and rubber, using the single input single output (SISO) impulse hammer method. A range of input force levels was used as the main method of exciting an observable NL response, defined as either a frequency shift of a given mode, or as a change of amplitude of response/input ratio of a mode as shown in standard FRF data plots. Lab level calibration of sensors was performed prior to testing, using the standard system calibration method [1], with a 3,030±0.5$gram$ mass.

All beams were 350(+0,-0.5)mm long and 30(+0,-0.5)mm wide. Aluminium 5083 beam components were 1, 2, 3 & 4mm thick, with 72GPa Young's Modulus, 0.33 Poisson's ratio and 2660kg/m^3 [10]. Nitrile rubber sheet component layers were 1 & 2mm thick, with

3GPa Young's Modulus, 0.5 Poisson's ratio and 1000kg/m^3 [11,12]. These material properties were used as the initial estimates, due to a lack of reliable supplier verified data, and later verified and updated against static and dynamic tests.

The modal analysis work used 11 different beam configurations, combining the individual components as listed in Table 1 with "A" and "R" indicating aluminium beams and rubber layers respectively, and the numbers representing their thicknesses in mm.

Table 1. Beam configurations used in modal testing and analysis, showing the beam components used for each layer.

Case No.	Configuration	Case No.	Configuration
1	A1	7	A4-A4
2	A2	8	A4-R1-A4
3	A3	9	A2-R1-A1-R2-A1-R1-A2
4	A4	10	A1-R2-A2-R2-A3
5	A1-R1-A1	11	A2-R2-A1-R2-A3
6	A1-R1-A1-R1-A1		

All beam configurations were rigidly clamped over one end, covering 50mm over the beam length. The beam layers were secured by 4 M3 bolts through 3.3mm⌀ holes located at 100, 170, 240 and 310mm from the end of the beam that is clamped. The clamp bolts were always tightened to 6Nm and beam bolts were tightened only by feel (no available torque wrenches could operate with such small bolt sizes), attempting to give consistent conditions for all tests.

The modal analysis specialist software MODENT was used to analyse the FRF test data obtained by using a National Instruments "Peripheral Component Interconnect eXtensions for Instrumentation" (PXI) platform, with simultaneous sampling, giving a frequency resolution of 0.2Hz. For each case, five force ranges were used, as shown in Table 2, and chosen to excite NL behaviour over as wide a range as possible, without damage to the beam, and whilst still achieving good quality coherence and repeatability. For each case, ten averages were taken and the impulse hammer force and accelerometer were located 60±5mm & 20.0±0.5mm respectively from the beam free end, on the beam top surface.

Table 2. Force ranges used in modal testing

Case No.	Force ranges (N)				
1	1-2	3-4	5-6	7-8	9-10
2	1-5	6-10	11-15	16-20	21-25
3	1-10	11-20	21-30	31-40	41-50
4	1-20	21-40	41-60	61-80	81-100
5	1-10	21-30	41-50	61-70	81-90
6	1-20	31-50	91-80	91-110	151-140
7	1-20	41-60	81-100	121-140	161-180
8	1-20	41-60	81-100	121-140	161-180
9	1-20	41-60	81-100	121-140	161-180
10	1-20	41-60	81-100	121-140	161-180
11	1-20	41-60	81-100	121-140	161-180

A linear FE model using ANSYS was used as a benchmark, as a further comparison to the test data, in order to identify NL behaviour. The model was verified against modal tests using the lowest input force levels and simplest beam configurations, as these would be expected to minimise the excitation and presence of NL behaviour, and hence most closely match linear behaviour. The model included a lumped mass to represent the added mass of the accelerometer. The FE model was also verified against static tests, by loading two beam configurations with a known mass, allowing extraction of relevant material properties. The static tests used the same clamping arrangement and torque settings

as for the modal tests, using configuration case numbers 4 & 8. Both were loaded using a 355.0±0.5*g* mass and a laser displacement sensor on the beam top surface located 60±1*mm* & 20.00±0.25*mm* respectively from the beam free end. The static model had the same clamping conditions and all other details as the dynamic model, except the accelerometer lumped mass was removed. The fundamental physics of the laser means its factory calibration is never altered unless there is a laser malfunction, so lab level calibration was not necessary, or indeed possible.

3. Results and Discussion

3.1 Calibration and measurement errors

Prior to lab level calibration, the modal hammer force sensor and accelerometers errors based on using their manufacturers supplied calibration certificates were a maximum of 2.2%. Correction of all sensor sensitivities after lab level calibration gave a maximum error of 0.18%. Their measurement errors were <3.0%. The laser displacement sensor had negligible calibration error, and due to factors such as surface incident angle and roughness, a measurement error of <0.5% was justifiable.

3.2 Static and dynamic model validation

Full details are not presented here as they are not the main focus of the work. However, comparing the static and dynamic experimental results to the initial models, led to the adjustment of the model material properties in order to try to optimise the error. This was difficult to achieve for the dynamic measurement case for higher modes, and it was decided to prioritise the first mode, as shown in Table 3. Blank cells indicate that the mode could not be observed in the measurements. The final material properties were

as follows: For the aluminium beams, 70.1*GPa* Young's Modulus, 0.33 Poisson's ratio and 2650*kg/m³*. For the rubber sheet, 5*GPa* Young's Modulus, 0.45 Poisson's ratio and 1000*kg/m³*.

Table 3. Percentage error, comparing the FE model predicted frequency to the dynamic tests measurements for the lower force ranges.

Case No.	Error (%)					
	Mode number					
	1	2	3	4	5	6
1	2.67	3.76	11.21	14.18	27.30	19.46
2	6.01	3.85	4.51	8.76	12.67	15.09
3	2.10	-1.07	-0.14	2.67	7.39	10.78
4	2.64	0.50	1.29	4.53		
5	7.73	7.85	15.17	29.51	-27.30	-12.22
6	8.08	-2.97	6.43	20.05		
7	3.37	6.27	12.62	22.36	39.33	41.41
8	3.39	-14.50	-12.14	-8.11		
9	1.34	-26.75	-21.36			
10	5.49	-23.18	-2.17			
11	1.22	-23.12	-15.70	-12.95	-4.44	

3.3 NL modal behaviour

Key results are shown in Tables 4 and 5, showing the measured frequencies and response mode peak amplitudes, for all eleven configurations and up to the first six modes. Each cell shows the absolute value (upper number) and the percentage difference (lower number; positive implies an increase, negative implies a decrease) when comparing the result of the highest force range to the lowest force range, for a given mode and beam configuration. For most configurations, if the trend shows an increase or decrease, then all intermediary force ranges also show an increase or decrease respectfully. For configurations where there is no consistent trend of increasing or decreasing amplitude or frequency shift, the cells include a " * " symbol. Given that the measurement error is <3.0%, for any shifts between -3% to +3%, no conclusion

can be drawn with respect to trends of increasing or decreasing amplitude or frequency. Blank cells indicate that it was not possible to observe the given mode number.

The general trends for a given configuration are that all beam configurations showed evidence of NL behaviour from the modal tests, with the FRF modes peak amplitudes and frequencies shifting for changes in the excitation force level. All modes for all sandwich beam configurations show decreasing peak amplitude and frequency, for increasing excitation force. The peak amplitude and frequencies for single beam configurations show a mix response to increasing the excitation force, with some modes increasing, some remaining unchanged, some decreasing and some not showing any clear trend.

Example FRF plots for selected cases are shown in Figs. 1-4. Each figure shows the trending of the shift of the mode peak amplitude and frequency, with the FRF measurement data curve shown for only the lower force range and for only one mode for clarity. Single points corresponding to the resonant peaks are only shown for all other forces ranges. The figure insert diagrams give a reminder of the beam configuration and thickness dimensions, with the solid black line indicating a rubber layer. Fig.1 shows an example of increasing amplitude and decreasing frequency, for increasing force range level. For this case, the trend line indicates there may be a limit point reached as the plotted points get successively closer together. No such detailed analysis was performed, and would be a topic of future work.

Table 4. Measured frequency absolute (upper number) and % shift values (lower number).

Case	Frequency (Hz and % shift)					
No.	Mode number					
	1	2	3	4	5	6
1	6.0	47.4	131.8	261.4	394.0	630.2
	0.00	-1.69	2.12	-0.46	2.99*	-0.06
2	13.4	96.6	283.0	548.2	885.4	1300.0
	0.00	1.04	-0.28	-1.13	0.38*	-3.92
3	22.4	156.8	451.6	879.0	1399.8	2030.4
	0.00	-0.26	-0.22	-0.27	0.11*	0.75*
4	30.6	207.6	593.8	1146.0		
	0.00	-0.19	0.00	-0.10		
5	18.8	98.6	210.8	307.2	772.2	983.2
	-4.26	-10.14	-13.19	-7.75	-14.94	-12.08
6	27.0	124.2	237.6	331.4		
	-3.70	-9.02	-14.56	-5.19		
7	62.8	380.8	973.6	1658.2	2163.8	3279.8
	0.00	-1.84	-9.10	-8.60	-4.13	-13.59
8	55.0	349.2	815.0	1400.8		
	-1.09	-4.18	-13.42	-5.34		
9	45.6	242.6	463.8			
	-5.70	-5.11	-9.66			
10	46.6	249.2	437.2			
	-3.43	-3.85	-23.74			
11	45.8	266.8	515.2	850.2	1161.0	
	-1.31	-4.72	-9.43	-9.95	-4.74	

Table 5. Measured peak response amplitude (upper number) and % shift values (lower number).

Case	Mode peak response amplitude (g /N and % shift)					
No.	Mode number					
	1	2	3	4	5	6
1	99.1	38.2	24.5	4.7	4.3	58.9
	35.68*	42.07	26.77*	-35.81	30.62	-21.48
2	96.05	29.55	84.63	14.22	9.15	27.42
	96.34	91.88	10.26*	60.78*	-69.17	-65.49
3	402.25	23.17	100.12	19.91	6.55	14.44
	-5.59	94.31*	46.72	49.11*	12.85	-44.54
4	538.89	49.43	222.59	34.43		
	-30.02	-76.91	-44.86	-42.46		
5	56.95	3.76	9.79	5.13	7.48	13.35
	-66.04	-27.22	-54.19	-61.67	-57.59	-65.72
6	26.61	3.82	4.49	2.90		
	-51.08	-47.34	-28.63	-40.91		
7	297.51	9.38	19.52	8.49	1.38	3.37
	-66.35	-80.34	-88.01	-79.51	-39.33	-75.05
8	14.64	1.86	2.62	2.68		
	-34.08	-31.69	-25.70	-40.16		
9	11.61	2.28	2.17			
	-45.55	-35.51	-33.63			
10	12.56	2.20	2.59			
	-28.06	-43.70	-36.17			
11	11.21	2.12	2.51	1.90	0.85	
	-23.70	-36.03	-34.16	-38.55	-64.80	

Fig. 2 shows an example of decreasing frequency and amplitude. The frequency shift is small and only for the first change of force level, and the amplitude shift also suggest a limit is

being reached. Fig. 3 shows no frequency shift and a less clear trend in decreasing amplitude.
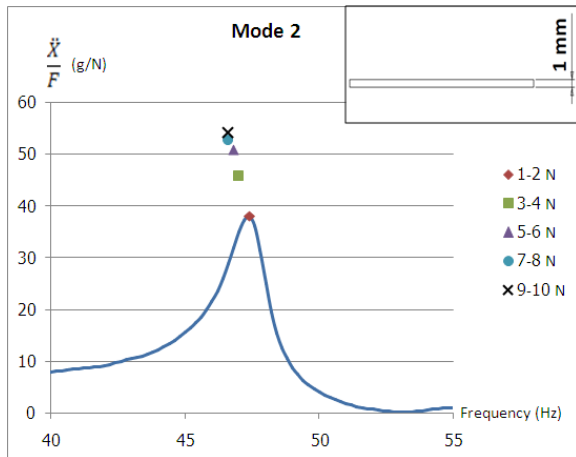
Figure 1: FRF measurement for case 1, mode 2.
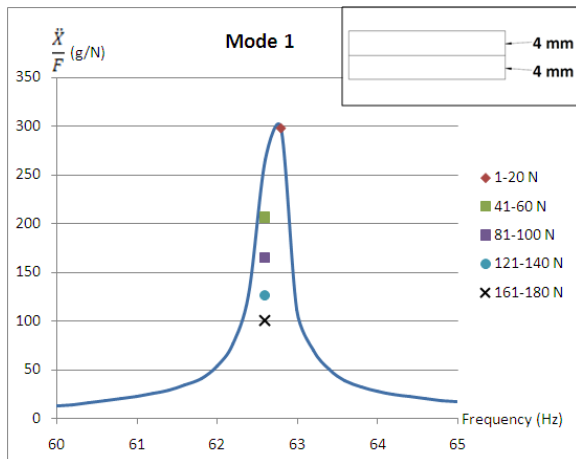
Figure 2: FRF measurement for case 7, mode 1.
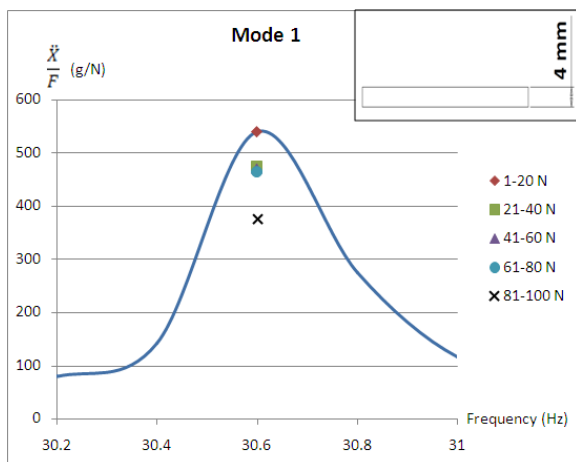
Figure 3: FRF measurement for case 4, mode 1.

Standard quality checks were performed on the FRF measured data, with a coherence of 0.9-1.0 for all modes except the 2nd mode for configuration case no. 9 which had a coherence

of 0.8. Given the modelling and experimental constraints of preferring to have one fixed location for the hammer and another for the accelerometer, as well as the number of modes sampled, some configuration cases had the hammer or accelerometer near a nodal line to within 2*mm*. For the accelerometer, this was cases 1 to 3, all for modes 5 and 6. For the hammer, this was case 3 mode 2. However, in general, the quality of the raw FRF data is believed to be sufficient for the key observations made in this work. In addition some FRF plots contained noise or a rough as opposed to a smooth curve, as shown in Fig. 4.
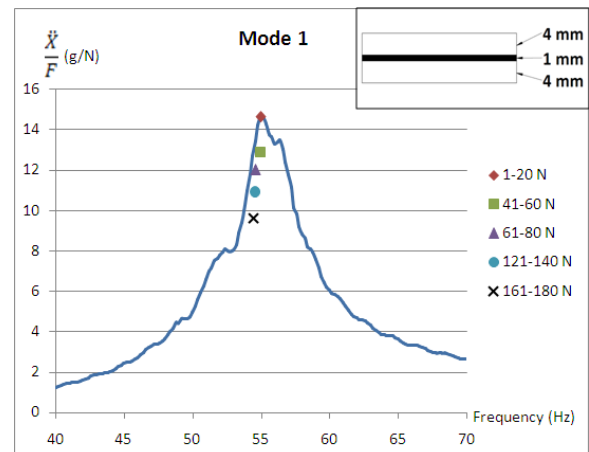
Figure 4: FRF measurement for case 8, mode 1.

This was only for some cases and modes where the response amplitude was very low, which could have been due to noise, but also may have been due to the possible additional effect of through thickness vibration modes for the sandwich structures. Standard modal analysis for normal modes assumes no such through thickness effect. The addition of the vibration of the layers, whereby the rubber effectively acts as a soft spring between the aluminium layers, will clearly reduce the amplitude response and frequency of what would otherwise be the normal mode. This is therefore a very strong source of

NL behaviour, and possibly the dominating source of NL behaviour as shown in these results for all sandwich structures. Given that it is only the single beams that sometimes show increasing and sometimes decreasing amplitude and/or frequency shifts, as the force range is increased, this might suggest there are some competing weak sources of NL behaviour, which are still present for sandwich configurations.

It is worth considering the effectiveness of the beam bolts. Ideally, the bolts should produce an effective infinite rigid joint between two beams, between two aluminium beams such as for configuration case 7, with no slip, no loss of contact and allowing full and effective transmission of forces as would be experienced by a solid equivalent 8mm thick single beam centreline. This would give 100% bolt effectiveness. In contrast, a 0% bolt effectiveness would mean the two 4mm beams essentially behave as two completely separate and out of contact beams, as if both were behaving as for configuration case 4. The results in Table 4 show the 1st mode frequencies for cases 4 and 7, being 30.6 and 62.8Hz respectively. If the bolt effectively was 0%, the result for case 7 would be the same as for case 4. The 1st mode frequency for a single solid 8mm beam can be estimated for identical test conditions, by extrapolating a best fit curve for the results for cases 1 to 4. In theory this should be a linear best fit line through the origin of thickness versus frequency, giving 63.64Hz with a "R-squared" value of 0.9987. Scaling the bolt effectiveness of 0% to 100% to match the frequency results of 30.6Hz (measured for case 4) and 63.64Hz (extrapolated prediction for a perfect equivalent 8mm thick beam), the

measured value of 62.8Hz for case 7 gives a bolt effectiveness of 97.5%. The same high bolt effectiveness could not be expected for sandwich beams with a rubber layer, as the rubber layer would allow relatively high shear and through thickness compression, and hence lead to a reduction in overall stiffness and bolt tension. Such effects would show up as strongly NL behaviour, in addition to the through thickness vibration behaviour suggested above.

Given the linear FE model predicted frequency percentage errors as shown in Table 3, the percentage shifts in Tables 4 and 5 can be used as an approximate indicator of the degree of observed NL behaviour. In some cases, the FE model percentage error is larger than the measured shift percentage and of the same sign, meaning the FE model cannot directly be used to prove the presence of NL behaviour or the degree of NL behaviour. In other cases, the magnitude may be greater but of the opposite sign, indicating the NL behaviour shift is in the opposite direction to the error and hence still a valid observation. However, the model accuracy for NL cases must be developed further. The measured data on its own is a sufficiently strong indicator of the presence and extent of NL behaviour. However, the output data includes the summed effect of all sources or types of non-linearity. Being able to systematically resolve and separate these effects is therefore a key next step in the research, and confirms the importance of experimental work that uses a wide range of structures and their component variations.

4. Conclusion

NL behaviour has been experimentally excited and observed in single and sandwich

aluminium and rubber layered beam configurations. The results suggest the presence of more than one source or type of non-linearity, sometimes with competing strong or weak effects, although these could not be independently isolated. Therefore further work should include isolating individual sources of non-linearity by developing experimental techniques as well as FE model development, ultimately aiming to be able to characterise and quantify each source and its predicted effect on measurements.

5. Acknowledgement

6. References

[1] Ewins, D.J., Modal Testing: Theory, Practice and Application. 2nd edition, ISBN: 0-86-380218-4, Research Studies Press Ltd., England, 2000.

[2] Edwards, J.H. (Editor), The Dynamic Testing Agency's Primer on Best Practice in Dynamic Testing. ISBN: 1-89-963016-3, Dynamic Testing Agency, 1993.

[3] Worden, K. and Tomlinson, G.R., Nonlinearity in Structural Dynamics: Detection, Identification and Modelling. 1st edition, ISBN: 0-75-030356-5, Taylor & Francis, 2001.

[4] Edwards, J.H. (Editor), The Dynamic Testing Agency's Handbook Volume 4: Non-linearity in Dynamic Testing, ISBN: 1-89-963007-4, Dynamic Testing Agency, 1993.

[5] Kerschen, G., et al., Past, Present and Future of Nonlinear System Identification in Structural Dynamics. *Mechanical Systems and Signal Processing*, Vol. 20, 2006, pp.505-592.

[6] Lee., Y.S., et al., Non-linear System Identification of the Dynamics of Aeroelastic Instability Suppression Based on Targeted Energy Transfers. *The Aeronautical Journal of the Royal Aeronautical Society*, Vol. 114, 2010, pp.61-82.

[7] Peeters, M., et al., Modal Testing of Nonlinear Vibrating Structures Based on Nonlinear Normal Modes: Experimental Demonstration. *Mechanical Systems and Signal Processing*, Vol. 25, 2011, pp.1227-1247.

[8] Carrella, A. and Ewins, D.J, Identifying and Quantifying Structural Nonlinearities in Engineering Application from Measured Frequency Response Functions. *Mechanical Systems and Signal Processing*, Vol. 25, 2011, pp.1011-1027.

[9] Mahmoodi, S.N., et al., An Experimental Investigation of Nonlinear Vibration and Frequency Response Analysis of Cantilevered Visco-elastic Beams. *J. of Sound & Vibration*, Vol. 311, 2008, pp.1409-1419.

[10] http://www.efunda.com

[11] http://www.matbase.com

[12] http://www.wikipedia.org